

OSCILLATIONS OF ROTOR SUPPORTED ON MAGNETIC BEARINGS WITH IMPACTS IN RETAINER BEARINGS

LADISLAV PŮST

*Institute of Thermomechanics, Academy of Sciences of Czech Republic, Prague, Czech Republic
e-mail: pust@it.cas.cz*

Dynamic properties of a rotor supported on two passive magnetic bearings are investigated by means of the numerical solution to the mathematical model of a prototype developed at the Institute of Thermomechanics ASCR. Magnetic supports always have to include the so-called retainer bearings in order to prevent the rotor from dangerous increase of oscillations due to damage in magnetic bearings. Retainer bearings are rolling bearings, the inner ring of which rotates after an oblique impact by the rotor journal. This rotation introduces an additional degree of freedom to the mathematical model of the rotor support. The main aim of this study is to gain the basic knowledge about the properties of such a system, therefore, a new model of impact motion with large amplitudes, introducing radial Hertz stiffness, material contact damping, tangential dry friction and viscous damping is developed. Dynamic properties of the system described by 6 differential equations containing strongly nonlinear terms are investigated, and the results are presented in form of response curves. Frequency intervals of periodic, quasi-periodic and chaotic motions are ascertained and effects of various parameters on the dynamic behavior of the studied system are determined.

Key words: space oscillations, passive magnetic bearing, rotor, retainer bearing, impact

1. Introduction

Magnetic bearings have been widely used due to a great variety of their advantages compared to conventional types of oil and roller bearings. Their unique advantages are: non-contact operation, lubricant-free working, possibility of high speed revolutions, zero drag against rotation, etc. There are two basic principles of magnetic bearings:

- Active Magnetic Bearings (AMB), which always require feedback control of the current and magnetic force for stable levitation of a rotor in the

given position. The very important advantage of the AMB is the tuning possibility for stiffness and damping in the radial direction by means of which dynamic properties of the whole rotor system can be easily changed, so that classical limitations can be overcome and reliability increased.

- Passive Magnetic Bearings (PMB) using strong permanent magnets are simpler than AMB because they do not need any feedback loops, any power amplifiers and no energy supply, but they have fixed stiffness and damping properties which cannot be controlled during operation. They have also very low radial damping and are more prone to exhibit unstable motions. In spite of this, PMB are very suitable for small machine aggregates, particularly for those with high angular velocities.

For safety reasons, all types of magnetic bearings have to contain central safety components, which are realized by emergency retainer bearings with a sufficient clearance between the shaft and inner ring of the rolling bearing. They protect magnetic bearings from direct contact with the rotor and retain amplitudes of vibrations within safe limits after their undesirable increase.

The present paper is oriented particularly on the investigation of dynamic behaviour of a rotor supported by a PMB after contact with the inner ring of the retainer bearing.

The rotor/stator rub is a very important problem of rotor dynamics and it has been investigated by lots of authors for many years, but mainly for the cases of rotor contact with the rigid, non-rotating inner surface of the stator (Goldman and Muszynska, 1994; Isaaksson, 1994; Wei Yang and Kikuan Tang, 1994). This occurs in rotating machinery like turbines, compressors, pumps, generators, etc., supported on conventional bearings. However, retainer bearings are usually ball or roller bearings, whose inner rings are set into rotation after oblique impacts with the rotor journal. The rotary motion is then damped by dry Coulomb friction in combination with viscous forces. Deformation of the radial contact is given by deformation between the shaft, inner ring, balls and the outer ring of the retainer bearing. Therefore, Hertz's law of the dynamic contact is used for description of radial forces in the PMB retainer bearings.

2. Passive magnetic bearing

A prototype of a rotor supported on two passive magnetic bearings has been designed and manufactured at the Institute of Thermomechanics, ASCR. The rotor has a mass of approximately 7 kg, and is provided on both ends with

three permanent magnetic rings $M1$ of a diameter $D = 60$ mm (Fig. 1a) magnetized in the axial direction. These rings are inserted into slots and matched with clearances between four similar magnetic rings $M2$ fastened in the stator (Púst *et al.*, 2003). The gap $d_1 = 0.5$ mm between the rings is constant during relative radial dislocation of the rings against each other. Deformation of magnetic lines produces the returning force F proportional to the radial displacement x (Fig. 1b). The retainer bearing Rb with a clearance $r_h = 0.5$ mm limits amplitudes of the shaft Sh in the resonance or at accidents. Because the rotor cannot be supported by permanent magnets in all directions, another type of support is used in the axial direction z . The stiff axial support As is drawn in Fig. 1a, however the axial active magnetic bearing is used in the real IT prototype.

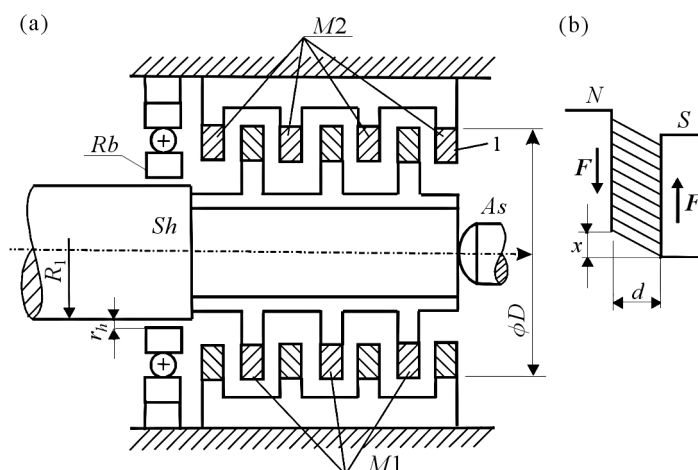


Fig. 1. Passive magnetic bearing with rolling retainer bearing

3. Spatial motion of the rotor

The first phase of investigation of rotor motion with impacts between the shaft and the inner ring was limited to one bearing only. The influence of various values of Hertz stiffness, combined with three types of damping of the tangential velocity of the ring was studied numerically by Púst and Kozánek (2002), Púst (2003). The obtained results are presented in form of response curves and trajectories of motion in the XY plane. Various kinds of impact motion were found – periodic with single or multiple periods, quasi-periodic and chaotic oscillations.

This paper presents a more exact dynamic model of rotor motion supported on two passive magnetic bearings and furnished with two retainer bearings. Motions in both bearings influence each other due to inertia of the rotor. Vertical and horizontal oscillations of the rotor differ by the weight mg which acts in the vertical direction. Motion in these two planes (x, z and y, z) is also connected by nonlinear properties of magnetic fields and nonlinear impact forces.

4. Differential equation of motion of the rotor

A stiff rotor in space has in general six degrees of freedom. In our case, the displacement in the z -axis is restricted by the axial bearing and can be neglected. Velocity of rotation around axis the z is assumed to be constant: $\omega_z = \omega$. The remaining 4 DOFs are described by displacements $x_1, x_2, y_1,$ and y_2 , in the points 1, 2 separated by the distance l . Both bearings are identical and they act on the rotor in points 1, 2 by forces $F_{x1}, F_{x2}, F_{y1}, F_{y2}$, (Fig. 2). Inertial properties of the rotor are defined by its mass m [kg] and moment of inertia I [kg m²] in the point T . The latter can be substituted by three masses m_1, m_2, m_3 in points 1, 2, 3.

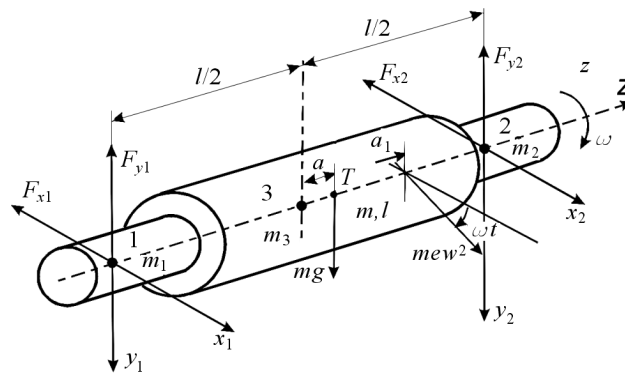


Fig. 2. Model of rotor

There are two main external forces which influence motion of the system. The force of gravity mg acts in the point T at a distance a measured from geometric centre 3. The exciting force (unbalance) can act in arbitrary position on the axis z . Let us suppose that the resultant $me\omega^2$ of the centrifugal forces acts at the distance a_1 from geometric centre 3. The substituted inertia masses are (Brepta *et al.*, 1994)

$$\begin{aligned}\frac{m_1}{m} &= -\frac{a}{l} + \frac{2a^2}{l^2} + \frac{2I}{l^2m} & \frac{m_2}{m} &= \frac{a}{l} + \frac{2a^2}{l^2} + \frac{2I}{l^2m} \\ \frac{m_3}{m} &= 1 - \frac{4a^2}{l^2} - \frac{4I}{l^2m}\end{aligned}\quad (4.1)$$

Equations of rotor motion are then

$$\begin{aligned}m_1\ddot{x}_1 + \frac{1}{4}m_3(\ddot{x}_1 + \ddot{x}_2) &= -F_{x1} + \left(\frac{1}{2} - \frac{a_1}{l}\right)m\epsilon\omega^2 \cos \omega t \\ m_2\ddot{x}_2 + \frac{1}{4}m_3(\ddot{x}_1 + \ddot{x}_2) &= -F_{x2} + \left(\frac{1}{2} + \frac{a_1}{l}\right)m\epsilon\omega^2 \cos \omega t \\ m_1\ddot{y}_1 + \frac{1}{4}m_3(\ddot{y}_1 + \ddot{y}_2) &= -F_{y1} + \left(\frac{1}{2} - \frac{a_1}{l}\right)m\epsilon\omega^2 \sin \omega t + \left(\frac{1}{2} - \frac{a}{l}\right)mg \\ m_2\ddot{y}_2 + \frac{1}{4}m_3(\ddot{y}_1 + \ddot{y}_2) &= -F_{y2} + \left(\frac{1}{2} + \frac{a_1}{l}\right)m\epsilon\omega^2 \sin \omega t + \left(\frac{1}{2} + \frac{a}{l}\right)mg\end{aligned}\quad (4.2)$$

where F_{xi} , F_{yi} ($i = 1, 2$) are the reaction forces in bearings, containing both magnetic and impact components. The subsystem of retainer bearings is presented in the plane x_1y_1 in Fig. 4. The displaced journal of the rotor touches the inner ring of the bearing in point A .

5. Rotor motion without impacts – small vibration

When displacements of the rotor journals are smaller than the clearance r_h , that is $r_i = \sqrt{x_i^2 + y_i^2} \leq r_h$, $i = 1, 2$, the only shearing component of the magnetic force acts on the rotor in its support. This force is centrally symmetrical and shows a softening characteristic with a weak cubic non-linearity

$$F = kr - k_3r^3$$

Components of this force in Cartesian coordinates are

$$F_{xi} = (k - k_3r_i^2)x_i \quad F_{yi} = (k - k_3r_i^2)y_i \quad i = 1, 2 \quad (5.1)$$

The damping of passive magnetic bearings itself is very low, close to zero. However, there are external damping forces from air drag, eddy currents, etc. Therefore, small linear damping $b\dot{x}_1$, $b\dot{x}_2$, $b\dot{y}_1$, $b\dot{y}_2$ must be added to the bearing forces F_{xi} , F_{yi} in the mathematical model of the bearings. The differential equations of rotor motion with 4 DOF in the case when the journals do not touch the retainer bearings are

$$\begin{aligned}
\left(m_1 + \frac{m_3}{4}\right)\ddot{x}_1 + \frac{m_3}{4}\ddot{x}_2 + b\dot{x}_1 + [k - k_3(x_1^2 + y_1^2)]x_1 &= \left(\frac{1}{2} - \frac{a_1}{l}\right)m\epsilon\omega^2 \cos \omega t \\
\left(m_2 + \frac{m_3}{4}\right)\ddot{x}_2 + \frac{m_3}{4}\ddot{x}_1 + b\dot{x}_2 + [k - k_3(x_2^2 + y_2^2)]x_2 &= \left(\frac{1}{2} + \frac{a_1}{l}\right)m\epsilon\omega^2 \cos \omega t \\
\left(m_1 + \frac{m_3}{4}\right)\ddot{y}_1 + \frac{m_3}{4}\ddot{y}_2 + b\dot{y}_1 + [k - k_3(x_1^2 + y_1^2)]y_1 &= \\
&= \left(\frac{1}{2} - \frac{a_1}{l}\right)m\epsilon\omega^2 \sin \omega t + \left(\frac{1}{2} - \frac{a}{l}\right)mg \\
\left(m_2 + \frac{m_3}{4}\right)\ddot{y}_2 + \frac{m_3}{4}\ddot{y}_1 + b\dot{y}_2 + [k - k_3(x_2^2 + y_2^2)]y_2 &= \\
&= \left(\frac{1}{2} + \frac{a_1}{l}\right)m\epsilon\omega^2 \sin \omega t + \left(\frac{1}{2} + \frac{a}{l}\right)mg
\end{aligned} \tag{5.2}$$

Inertial properties of the rotor (m , I , a) have been determined very easily from the real structure by a simple identification procedure or from its drawings. The prototype made at the Institute of Thermomechanics is shown in Fig. 3. The left pedestal contains also an axial active magnetic bearing. Axial motion of the rotor is measured at the right pedestal. The rotor prototype has a mass $m = 7.379$ kg, moment of inertia with respect to the axis x going through the centre of gravity T is $I = 945.7$ kg cm² and the shift of the centre of gravity along the axis z is $a = 0.5$ mm. The distance between the centres of magnetic bearings is $l = 352$ mm.

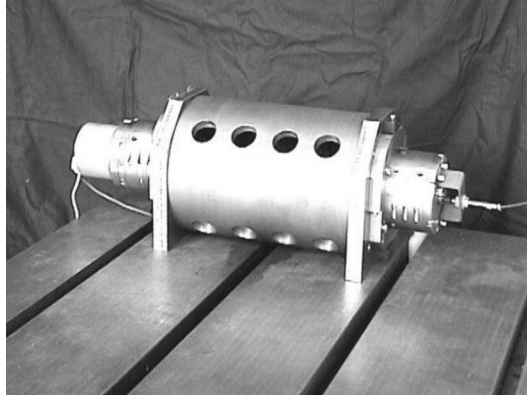


Fig. 3. Experimental test rig at Institute of Thermomechanics (ASCR)

Measurements of radial vibration can also be used for the identification of unknown stiffness and damping parameters of the permanent magnetic radial support after its assembling. Two complex eigenvalues of the stiff rotor were identified from the response

$$-2.4 + 28.5i \text{ Hz} \quad \text{and} \quad -2.5 + 46i \text{ Hz} \tag{5.3}$$

The corresponding linear stiffness of magnetic bearings is $k = 1.25 \cdot 10^5 \text{ kg s}^{-2}$ and the averaged damping coefficient is $b = 45.8 \text{ kg s}^{-1}$.

6. Impacts in retainer bearings

The aim of this Section is to gain basic information about the type of rotor motion when the rotor is subjected to impacts in the retainer bearings. Because parameters of impacts (k_h , b_h , f , b_4 , etc.) are unknown so far, numerical simulations have been carried out in dimensionless values. Such form of results is most general; it describes behaviour of a wide class of rotor systems. Properties of a real structure can be determined very easily from dimensionless results by simple multiplication.

During operation of the rotor, particularly in resonance, at transient motion etc., impacts in the retainer bearing can occur, and therefore, a strongly nonlinear mathematical model is required to describe motion of the rotor system. The beginning of contact is shown in Fig. 4, where the rotor (radius R_1) touches in point A the inner ring of the retainer bearing. The cause of the damping of the inner ring (mass m_4) during motion against the outer ring of the retainer bearing is the rolling resistance of balls and the viscous resistance of the lubricant. Therefore, the coefficient b_4 of viscous damping and the constant dry friction force F_d is introduced into the mathematical model.

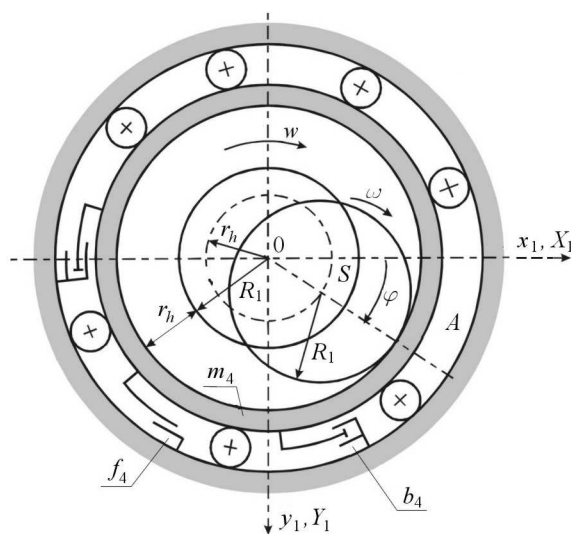


Fig. 4. Safety retainer bearing with deflected journal

The inner ring of the retainer bearing rotates with the velocity w after an oblique impact and the mathematical model must respect both radial deformation of the bearing and tangential forces arising at the contact between the rotor rotating with an angular velocity ω and the inner ring having another velocity. Mathematical models of the supports must contain differential equations of inner rings.

A dynamic Hertz's contact force

$$F_r = k_h(r - r_h)^{\frac{3}{2}} \left[1 + \frac{b_h}{r}(\dot{x}x + \dot{y}y) \right]$$

is supposed to express the radial component of the force. Dry friction with the coefficient f in contact describes the tangential component of the force between the journal and inner ring

$$F_\tau = F_r f \operatorname{sgn} \left[\frac{1}{r}(\dot{y}x - \dot{x}y) + R_1\omega - w \right] \quad r = \sqrt{x^2 + y^2}$$

where k_h , b_h are Hertz's contact coefficients, $w_r = \dot{x} \cos \varphi + \dot{y} \sin \varphi = (\dot{x}x + \dot{y}y)/r$ and $w_t = \dot{y} \cos \varphi - \dot{x} \sin \varphi = (\dot{y}x - \dot{x}y)/r$ are radial and tangential velocities of the rotor, w [m s^{-1}] is the circumferential velocity of the inner retainer bearing ring.

In this case, the support forces F_{xi} , F_{yi} ($i = 1, 2$) in equations (4.1) contain, except for linear and weakly nonlinear terms $b\dot{x}_i + [k - k_3(x_i^2 + y_i^2)]x_i, \dots$ (see (6.1)), also strong nonlinear impact forces with vertical $F_{x_{imp}}$ and horizontal $F_{y_{imp}}$ components ($i = 1, 2$)

$$\begin{aligned} F_{x_{imp}} &= A_i \left(\frac{x_i}{r_i} - \frac{y_i}{r_i} B_i \right) \\ F_{y_{imp}} &= A_i \left(\frac{y_i}{r_i} + \frac{x_i}{r_i} B_i \right) \end{aligned} \quad (6.1)$$

where for $i = 1, 2$

$$\begin{aligned} r_i &= \sqrt{x_i^2 + y_i^2} \\ A_i &= H(r_i - r_h) F_{ri} = H(r_i - r_h) k_h (r_i - r_h)^{\frac{3}{2}} \left[1 + \frac{b_h}{r_i} (\dot{x}_i x_i + \dot{y}_i y_i) \right] \\ B_i &= f \operatorname{sgn} \left(\frac{1}{r_i} (\dot{y}_i x_i - \dot{x}_i y_i) + R_1 \omega - w_i \right) \end{aligned}$$

The velocities w_1 , w_2 are given by additional two equations (6.3) describing motion of the inner rings of retainer bearings.

While solving, Heaviside's functions $H(r_i - r_h)$ switch-on or switch-off the multiplied expressions of impact forces into equations in question. Heaviside's function is $H = 1$ if $r_i > r_h$ and $H = 0$ if $r_i \leq r_h$.

The complete set of equations describing spatial motion of the stiff rotor supported on passive magnetic bearings with the retainer bearings is

$$\begin{aligned}
m_1\ddot{x}_1 + \frac{m_3}{4}(\ddot{x}_1 + \ddot{x}_2) + b\dot{x}_1 + (k - k_3r_1^2)x_1 + A_1\left(\frac{x_1}{r_1} - \frac{y_1}{r_1}B_1\right) &= \\
= \left(\frac{1}{2} - \frac{a_1}{l}\right)m\epsilon\omega^2 \cos \omega t & \\
m_2\ddot{x}_2 + \frac{m_3}{4}(\ddot{x}_1 + \ddot{x}_2) + b\dot{x}_2 + (k - k_3r_2^2)x_2 + A_2\left(\frac{x_2}{r_2} - \frac{y_2}{r_2}B_2\right) &= \\
= \left(\frac{1}{2} + \frac{a_1}{l}\right)m\epsilon\omega^2 \cos \omega t & \\
m_1\ddot{y}_1 + \frac{m_3}{4}(\ddot{y}_1 + \ddot{y}_2) + b\dot{y}_1 + (k - k_3r_1^2)y_1 + A_1\left(\frac{y_1}{r_1} + \frac{x_1}{r_1}B_1\right) &= \\
= \left(\frac{1}{2} - \frac{a_1}{l}\right)m\epsilon\omega^2 \sin \omega t + \left(\frac{1}{2} - \frac{a}{l}\right)mg & \\
m_1\ddot{y}_2 + \frac{m_3}{4}(\ddot{y}_1 + \ddot{y}_2) + b\dot{y}_2 + (k - k_3r_2^2)y_2 + A_2\left(\frac{y_2}{r_2} + \frac{x_2}{r_2}B_2\right) &= \\
= \left(\frac{1}{2} + \frac{a_1}{l}\right)m\epsilon\omega^2 \sin \omega t + \left(\frac{1}{2} + \frac{a}{l}\right)mg &
\end{aligned} \tag{6.2}$$

and

$$\begin{aligned}
m_4\dot{w}_1 + b_4w_1 + F_{d1}H(w_1) - A_1B_1 &= 0 \\
m_4\dot{w}_2 + b_4w_2 + F_{d2}H(w_2) - A_2B_2 &= 0
\end{aligned} \tag{6.3}$$

where for $i = 1, 2$

$$F_{di} = f_4F_{ri}$$

By introducing non-dimensional variables and parameters for linear and weakly nonlinear parts of the rotor system

$$\begin{aligned}
\alpha &= \frac{2a}{l} & \alpha_1 &= \frac{2a_1}{l} & \delta &= \frac{mg}{2kr_h} & X_i &= \frac{x_i}{r_h} \\
Y_i &= \frac{y_i}{r_h} & ec &= \frac{e}{2r_h} & \tau &= t\sqrt{\frac{k}{m}} & \eta &= \omega\sqrt{\frac{m}{k}} \\
B &= \frac{b}{\sqrt{km}} & \kappa &= -r_h^2\frac{k_3}{k} & \rho^2 &= \frac{4I}{ml^2} \\
\mu_1 &= \frac{m_1}{m} = \frac{1}{2}(-\alpha + \alpha^2 + \rho^2) & \mu_2 &= \frac{m_2}{m} = \frac{1}{2}(\alpha + \alpha^2 + \rho^2) \\
\mu_{34} &= \frac{m_3}{4m} = \frac{1}{4}(1 - \alpha^2 - \rho^2)
\end{aligned} \tag{6.4}$$

and for impacts and retainer bearings

$$\begin{aligned}
\kappa_h &= K_h \frac{\sqrt{r_h}}{k} & B_h &= b_h \sqrt{km} & \mu_4 &= \frac{m_4}{m} \\
B_4 &= b_4 \sqrt{km} & \rho_0 &= \frac{R_1}{r_h} & \Phi_{di} &= \frac{F_{di}}{hr_h} \\
\rho_1 &= \frac{r_1}{r_h} = \sqrt{X_1^2 + Y_1^2} & \rho_2 &= \frac{r_2}{r_h} = \sqrt{X_2^2 + Y_2^2} & v &= \frac{w}{r_h} \sqrt{\frac{m}{k}} \\
H(r_1 - r_h) &= H(\rho_1 - 1)
\end{aligned} \tag{6.5}$$

we get a simpler form of differential equations of rotor motion, convenient for numerical solution

$$\begin{aligned}
&(\mu_1 + \mu_{34})X_1'' + \mu_{34}X_2'' + BX_1' + X_1(1 + \kappa\rho_1^2) + \\
&\quad + H(\rho_1 - 1)\kappa_h(\rho_1 - 1)^{\frac{3}{2}}[1 + B_h(X_1'X_1 + Y_1'Y_1)] \cdot \\
&\quad \cdot [X_1 - Y_1 f \operatorname{sgn}(Y_1'X_1 - X_1'Y_1 + \rho_0\eta - v_1)] = (1 - \alpha_1)ec\eta^2 \cos \eta\tau \\
&(\mu_2 + \mu_{34})X_2'' + \mu_{34}X_1'' + BX_2' + X_2(1 + \kappa\rho_2^2) + \\
&\quad + H(\rho_2 - 1)\kappa_h(\rho_2 - 1)^{\frac{3}{2}}[1 + B_h(X_2'X_2 + Y_2'Y_2)] \cdot \\
&\quad \cdot [X_2 - Y_2 f \operatorname{sgn}(Y_2'X_2 - X_2'Y_2 + \rho_0\eta - v_2)] = (1 + \alpha_1)ec\eta^2 \cos \eta\tau \\
&(\mu_1 + \mu_{34})Y_1'' + \mu_{34}Y_2'' + BY_1' + Y_1(1 + \kappa\rho_1^2) + \\
&\quad + H(\rho_1 - 1)\kappa_h(\rho_1 - 1)^{\frac{3}{2}}[1 + B_h(X_1'X_1 + Y_1'Y_1)] \cdot \\
&\quad \cdot [Y_1 - X_1 f \operatorname{sgn}(Y_1'X_1 - X_1'Y_1 + \rho_0\eta - v_1)] = (1 - \alpha_1)ec\eta^2 \sin \eta\tau + (1 - \alpha)\delta \\
&(\mu_2 + \mu_{34})Y_2'' + \mu_{34}Y_1'' + BY_2' + Y_2(1 + \kappa\rho_2^2) + \\
&\quad + H(\rho_2 - 1)\kappa_h(\rho_2 - 1)^{\frac{3}{2}}[1 + B_h(X_2'X_2 + Y_2'Y_2)] \cdot \\
&\quad \cdot [Y_2 - X_2 f \operatorname{sgn}(Y_2'X_2 - X_2'Y_2 + \rho_0\eta - v_2)] = (1 + \alpha_1)ec\eta^2 \sin \eta\tau + (1 + \alpha)\delta
\end{aligned} \tag{6.6}$$

and

$$\begin{aligned}
&m_4v_1' + B_4v_1 + \Phi_{d1}H(v_1) - H(\rho_1 - 1)f\kappa_h(\rho_1 - 1)^{\frac{3}{2}}[1 + B_h(X_1'X_1 + Y_1'Y_1)] \cdot \\
&\quad \cdot \operatorname{sgn}(Y_1'X_1 - X_1'Y_1 + \rho_0\eta - v_1) = 0 \\
&m_4v_2' + B_4v_2 + \Phi_{d2}H(v_2) - H(\rho_2 - 1)f\kappa_h(\rho_2 - 1)^{\frac{3}{2}}[1 + B_h(X_2'X_2 + Y_2'Y_2)] \cdot \\
&\quad \cdot \operatorname{sgn}(Y_2'X_2 - X_2'Y_2 + \rho_0\eta - v_2) = 0
\end{aligned} \tag{6.7}$$

Numerical solution of the set of six equations (6.6) and (6.7) has been carried out with the help of the Runge-Kutta integration method. Numerical simulations enable one to analyse spatial motion of the rotor, particularly in the cases of contact between the stiff rotor and one or both retainer bearings.

As an example, let us show response curves of a rotor with parameters

$$\begin{aligned} \alpha = \frac{2a}{l} = 0.01 & & \alpha_1 = \frac{2a_1}{l} = -0.3 & & \rho^2 = \frac{4I}{ml^2} = 0.96 \\ \frac{R_1}{r_h} = 100 & & \kappa = -0.001 & & \end{aligned} \quad (6.8)$$

The retainer bearings are characterised by the following dimensionless data

$$\begin{aligned} \kappa_h = k_h \frac{\sqrt{r_h}}{k} = 10 & & B_h = \frac{b_h}{\sqrt{km}} = 1.5 & & f = 0.2 \\ f_4 = 0 & & \mu_4 = \frac{m_4}{m} = 0.01 & & B_4 = \frac{b_4}{\sqrt{km}} = 0.1 \end{aligned} \quad (6.9)$$

The effect of different eccentricities e of the rotor mass is given by the following values of the dimensionless parameter $ec = e/(2r_h) = 0.005; 0.01; 0.015$.

Vibrations of a well-balanced rotor with the eccentricity $ec = 0.005$ does not reach the value of the retainer bearing clearance r_h , and the dimensionless maximum amplitudes X_m, Y_m are always less than 1, see Fig. 5. The system behaves as a linear one.

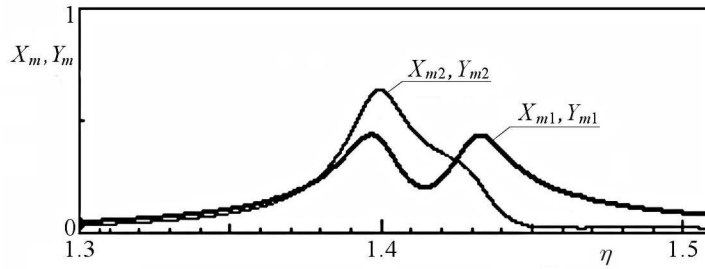


Fig. 5. Response curves of well balanced rotor; $ec = 0.005$

Two times higher unbalance $ec = 0.01$ causes larger amplitudes that result in impacts in the retainer bearings (Fig. 6 and Fig. 7). In these figures, response curves of motion in the horizontal direction x (amplitudes X_m), at slowly increasing frequency η (15 000 periods in $\Delta\eta = 0.3$) are shown in the upper half of the pictures, while the vertical amplitudes Y_m are displayed in the bottom half. Thick lines represent amplitudes of bearing No. 1, those of bearing No. 2 are indicated by thin lines. The frequency step is very low, the increase of η by 1% lasts 500 periods. Therefore, the oscillations can be considered as quasi-stationary.

The response curves in the upper (horizontal) and bottom (vertical) parts differ very moderate by due to a very low value of the static deformation δ .

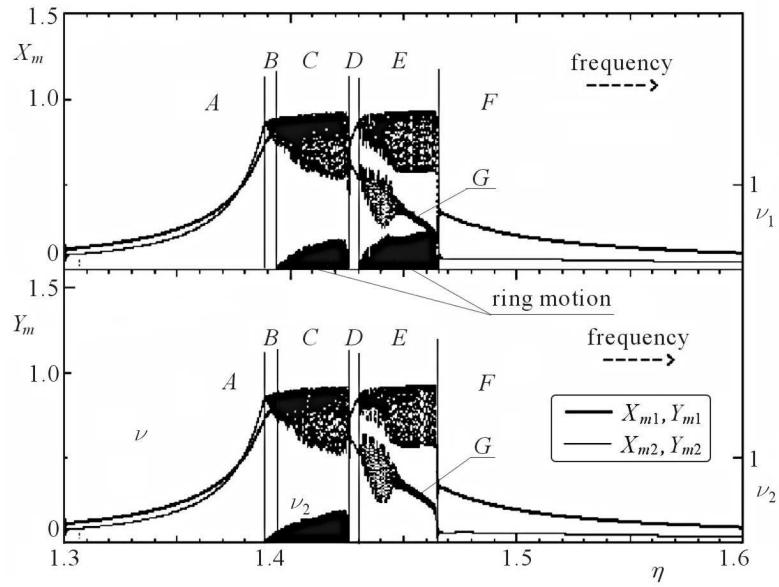


Fig. 6. Response curves of rotor with eccentricity $ec = 0.01$. Increasing frequency η

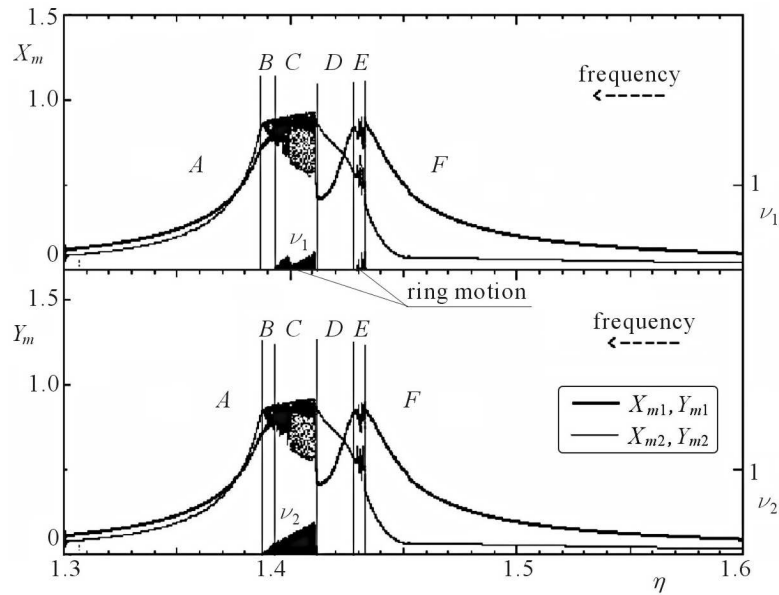


Fig. 7. Response curves of rotor with eccentricity $ec = 0.01$. Decreasing frequency η

Large differences are seen in the courses of motions of the inner rings $v_1(\eta)$ and $v_2(\eta)$, characterized by black areas near the axis η . The scale of velocities v is on the right side of the diagram.

Several types of rotor oscillations can be ascertained during the increase of the excitation frequency η . The range A ($1.300 < \eta < 1.389$), D ($1.425 < \eta < 1.430$), and F ($1.464 < \eta$) in Fig. 6 correspond to oscillations without impacts in the retainer bearings. In the range B ($1.389 < \eta < 1.393$), impacts in bearing No. 2 arise. Impacts in bearing No. 1 only occur in the range E ($1.430 < \eta < 1.464$). The range C ($1.393 < \eta < 1.425$) is characterized by impacts in both retainer bearings. These impacts cause interrupted revolutions of the bearing rings.

The impacts also change forms of the response curves $X_m(\eta)$, $Y_m(\eta)$. In the range C , impacts in both bearings change periodic oscillations into quasi-periodic ones or chaotic motion. A similar type of oscillations exists also in the range E , but impacts occur only in bearing No. 1, while in bearing No. 2, only irregular impact-less oscillations are observed.

The response curves at the decreasing frequency η (Fig. 7) are very different from the response curves at the increasing frequency. The areas of periodic impact-less motions A , D , F are wider, and the areas of irregular motions C , E are very narrow. Also, interrupted revolutions ν_1 , ν_2 of the bearing rings have lower velocities.

Further increase of eccentricity $ec = 0.015$ (Fig. 8) results into enlargement of the area C with quasi-periodic and chaotic motions, where impacts occur in both bearings. For such a large eccentricity, the impact-less area A does not change considerably, the area F changes a little more, but the area D disappears completely.

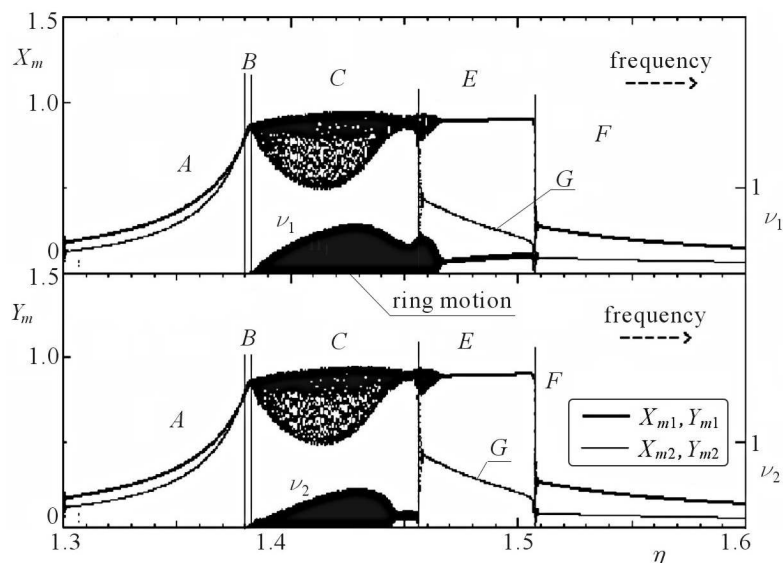


Fig. 8. Response curves of rotor with eccentricity $ec = 0.015$. Increasing frequency η

Irregular motion in the area E exists only at the left margin, but then the motion stabilizes on periodic oscillations, which in bearing No. 1 is given by revolution with continuous contact between the rotor and the inner ring of the bearing.

No contact appears in bearing No. 2, and the amplitudes X_{m2} and Y_{m2} decrease along the curves G . At a frequency of $\eta = 1.507$, this type of motion jumps into regular periodic impact-less vibration F .

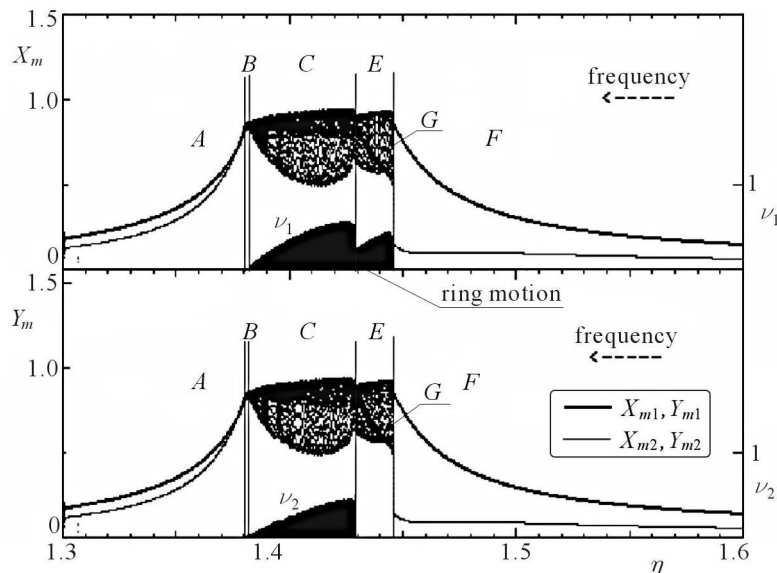


Fig. 9. Response curves of rotor with eccentricity $ec = 0.015$. Decreasing frequency η

The response curves at the decreasing frequency η and for the high eccentricity $ec = 0.015$ are shown in Fig. 9. Intervals of η labelled C and E are smaller than those in Fig. 8, and no oscillations with continuous revolution v_1 , v_2 of the inner rings of the retainer bearings occur. Impact-less oscillations F convert into chaotic oscillations E with impacts in bearing No. 1 after the dimensionless amplitude Y_{m1} reaches value 1. At the same time, the amplitude Y_{m2} jumps on this boundary to an approximately three times higher value and continues along the curve G (it is overlapped in Fig. 9 by records of irregular oscillations Y_{m1}). This amplitude reaches value 1 on the boundary between C and E regions and turns into irregular oscillations connected with the interrupted revolutions v_2 (see the bottom part of the region C). This type of oscillations extends up to the field B , where the inner ring of bearing 1 does not rotate ($v_1 = 0$). Only ring 2 rotates intermittently, but with a very low velocity. Large viscosity forces in the retainer bearings were supposed in that example, and therefore the case of the rotor rotating together with the inner ring did not occur.

Motion of such a complicated system is influenced by many parameters. There are 12 parameters in expressions (6.8) and (6.9). Because the radial stiffness of passive magnetic bearings is not too high, it is worth to examine the effect of weight on oscillations of the rotor.

Suppose that the rotor weight acts in the centre of a symmetric system ($a = 0$) and causes a vertical shift $y_T = mg/(2k)$, where k is the stiffness of one magnetic bearing. This shift reduces the gap in the retainer bearing and can cause undesired impacts of the rotor journal and the inner ring. Therefore, the magnetic bearing box is separated from the stator in which the retainer bearing is fastened. Then the vertical shift y_T can be eliminated by a suitable inverse shift of magnetic bearings pedestals so that the equilibrium position of the rotor axis coincides with the axis of the retainer bearing. In consequence, the centre of magnetic field is shifted by $y_T = -mg/(2k)$ with respect to the rotor (and retainer bearing) axis. This weight-shift in the prototype IT-ASCR is 0.3 mm, which is 60% of the clearance $r_h = 0.5$ mm. Due to errors in setting up to the exact position of the magnetic bearing support, some residual shift can remain between the axis of the retainer bearing and the rotor axis. The situation (Fig. 10) is described by

$$y_d = y_T - y_s$$

where

- y_T – static deflection due to weight, $y_T = mg/(2k)$
- y_s – shift of the bearing support, $y_s = \alpha y_T$
- y_d – resultant deflection of the rotor axis with respect to the retainer bearing axis.

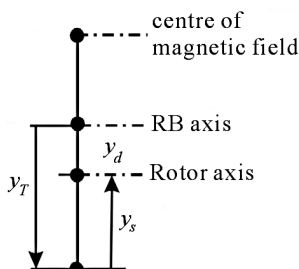


Fig. 10. Elimination of weight

After adjustment elimination of the weight-shift, the axis of the retainer bearing coincides with the rotor axis, but the magnetic field axis is moved upwards.

The response curves of the maximum amplitudes $X_{m1}, X_{m2}, Y_{m1}, Y_{m2}$ versus the excitation frequency $\eta = \omega\sqrt{m/k}$ and curves of velocities v_1, v_2 are

plotted in the upper part of Fig. 11 for the following parameters $R_1 = 40r_h$, $e = 0.03r_h$, $k_h = 50k\sqrt{r_h}$, $b_h = 3\sqrt{km}$, $f = 0.15$, $b_4 = 0.03\sqrt{km}$ (other parameters are the same as in (6.8)) and for 90% elimination of the weight effect ($\alpha = 0.9$).

The left part of the upper half of Fig. 11 consists of 6 sections; the first three describe the properties of left bearing 1, the last three correspond to right bearing 2.

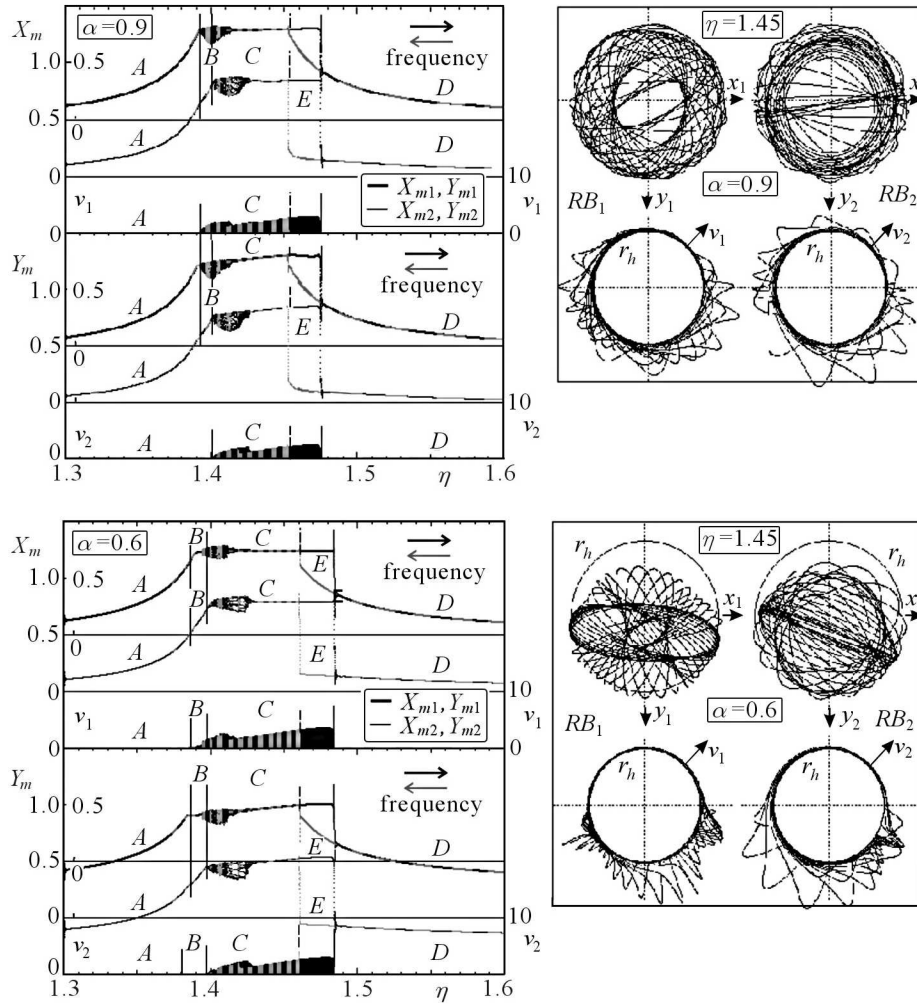


Fig. 11. Upper half: response curves and trajectories of journal centres S and polar diagrams with radius $r = r_h + v_i$, $i = 1, 2$, where v_i – velocity of inner rings, $\alpha = 0.9$. Lower half: response curves and trajectories of journal centres S and polar diagrams of velocity v , but for $\alpha = 0.6$

There are several types of rotor oscillations during a very slow increase of the excitation frequency. Oscillations without impacts are in the range A , D . In the range B , impacts in bearing 1 appear. Impacts in both bearings and chaotic motion occur in the range C together with interrupted revolution of both retainer bearing rings. In the second half of the range C , interrupted motions v_1, v_2 change into monotonous rotation, and the rotor is in permanent contact with the retainer bearings. At $\eta = 1.483$, the motion jumps into free contact-less rotation in the range D . The response curves at the reverse frequency trend are drawn in grey colour. In the frequency zones, where the records for increasing and decreasing frequency overlap, the grey record is interrupted (see grey strips in the range C).

Trajectories of the journal centres S at the frequency $\eta = 1.45$, where impacts in both bearings occur, are in the upper right corner. Polar diagrams with the radius $r = r_h + v_i$, $i = 1, 2$ in the lower part describe velocities of the inner rings of the retainer bearings.

Plots in the bottom half of Fig. 11 describe properties of rotor motion for the large effect of weight: $\alpha = 0.6$. The response curves x_m, η are similar, but the curves for vertical oscillations y_m, η are shifted downwards. The trajectories on the left side show this shift, the impacts occur particularly on the bottom part of the bearing rings.

7. Conclusion

- A mathematical model of spatial oscillations of a stiff rotor supported on two passive radial magnetic bearings has been derived at first for a weakly nonlinear system.
- The new mathematical model of rotor motion with impacts in the retainer bearings has been derived in form of six differential equations containing strong nonlinear terms – Hertz's dynamic contacts, dry friction, etc.
- Two equations of revolution of the inner rings of ball bearings have been added to the four equations of rotor motion.
- Examples of response curves for various excitations defined by the relative mass eccentricity $ec = e/(2r_h)$ (r_h is the clearance in the retainer bearings) proved that horizontal and vertical oscillations differ due to the effect of weight.

- Numerical solution enables one to find regions of the frequency η where the rotor oscillates without impacts, with impacts in the left bearing, with impacts in the right one or in both bearings.
- The inner rings of the retainer bearings rotate according to the intensity of impacts either with interruptions or continuously.
- Amplitudes of quasi-periodic impact motion of the rotor are determined and limited by clearances in the retainer bearings.
- Due to the large effect of weight on the equilibrium position, elimination of this shift is very important.

Acknowledgement

This work was carried out in the frame of project GA CR No. 101/06/1787.

Note: This article is extended paper [6].

References

1. BREPTA R., PŮST L., TUREK F., 1994, *Mechanical Vibrations* (in Czech, TP71), Sobotáles, Prague, pp. 589
2. GOLDMAN P., MUSZYNSKA A., 1994, Chaotic behavior of rotor/stator systems with rubs, *Transactions ASME, J. of Vibration and Acoustics*, **116**, 692-701
3. ISAAKSSON J.L., 1994, Chaotic response of rotor/stator rubs, *Proc. 4. International Conference on Rotor Dynamics*, Chicago, 91-95
4. KUDRA G., AWREJCEWICZ J., 2003, The triple pendulum with barriers as a first step in modelling of the piston-connecting rod-crankshaft system, *Proceedings 7th Conference on Dynamical Systems, Theory and Applications*, Lodz, Awrejcewicz J., Owczarek A., Mrozowski J. (edit.), **1**, 199-206
5. PŮST L., 2003a, Dynamical properties of passive magnetic bearing, *Engineering Mechanics*, **10**, 1, 1-16
6. PŮST L., 2003b, Space oscillations of rotor supported on magnetic bearings with impacts in retainer bearings, *Proceedings 7th Conference on Dynamical Systems, Theory and Applications*, Lodz, Awrejcewicz J., Owczarek A., Mrozowski J. (edit.), **1**, 65-84
7. PŮST L., KOZÁNEK J., 2002, Vibration of rotor supported in magnetic bearing with impact, *Proc. Engineering Mechanics*, Svratka, VUT Brno, edition CD ROM, 10

8. PŮST L., KOZÁNEK J., VESELÝ J., 2003, Rotor supported on magnetic bearings – numerical and experimental analysis, *Engineering Mechanics*, **10**, 5, 345-358
9. WEI YANG, KIKUAN TANG, 1994, Chaotic response of rotor/stator rubs, *Proc. 4. International Conference on Rotor Dynamics*, Chicago, 91-95

Oscylacje wirnika podpartego w łożyskach magnetycznych wywołane obciążeniem udarowym łożyska ustalającego

Streszczenie

Dynamiczne właściwości wirnika podpartego w dwóch pasywnych łożyskach magnetycznych zbadano w drodze symulacji numerycznych matematycznego modelu prototypu zbudowanego w Instytucie Termomechaniki Akademii Nauk Czeskiej Republiki. Podpory magnetyczne zawsze muszą zawierać w swej strukturze tzw. łożyska ustalające, które zapobiegają przed gwałtownym wzrostem drgań wywołanych uszkodzeniem łożysk magnetycznych. Łożyska ustalające są łożyskami tocznymi, których wewnętrzny pierścień zaczyna się obracać po ukośnym uderzeniu czopa wirnika. To z kolei wprowadza dodatkowy stopień swobody do modelu. Głównym celem analizy jest uzyskanie wiedzy na temat właściwości takiego układu, dlatego też zbudowano nowy model odzwierciedlający ruch po udarze o dużej amplitudzie i uwzględniający promieniową sztywność Hertza, tłumienie materiałowe w strefie kontaktu, tarcie suche styyczne i tłumienie wiskotyczne. Właściwości dynamiczne układu opisano 6 równaniami różniczkowymi ruchu zawierającymi człony nieliniowe. Rozwiązanie zaprezentowano w formie wykresów odpowiedzi układu. Stwierdzono występowanie przedziałów częstości odpowiadających ruchowi okresowemu, quasi-okresowemu oraz chaotycznemu. Określono też wpływ wielu parametrów układu na jego dynamikę.

Manuscript received August 3, 2006; accepted for print October 18, 2006